Pyridoxamine Analogues Scavenge Lipid-Derived γ-Ketoaldehydes and Protect against H 2 O 2 -Mediated Cytotoxicity †

ARTICLE *in* BIOCHEMISTRY · JANUARY 2007

Impact Factor: 3.02 · DOI: 10.1021/bi061860g · Source: PubMed

Published in final edited form as:
Biochemistry. 2006 December 26; 45(51): 15756–15767. doi:10.1021/bi061860g.

PYRIDOXAMINE ANALOGS SCAVENGE LIPID-DERIVED γ-KETOALDEHYDES AND PROTECT AGAINST H_2O_2-MEDIATED CYTOTOXICITY†

Sean S. Davies[*,‡], **Eric J. Brantley**[‡], **Paul A. Voziyan**[§], **Venkataraman Amarnath**[‖], **Irene Zagol-Ikapitte**[‡], **Olivier Boutaud**[‡], **Billy G. Hudson**[§], **John A. Oates**[‡,⊥], and **L. Jackson Roberts II**[‡,⊥]

‡*Department of Pharmacology, Vanderbilt University, Nashville, TN 37232*

⊥*Department of Medicine, Vanderbilt University, Nashville, TN 37232*

‖*Department of Pathology, Vanderbilt University, Nashville, TN 37232*

§*Department of Nephrology, Vanderbilt University, Nashville, TN 37232*

Abstract

Isoketals and levuglandins are highly reactive γ-ketoaldehydes formed by oxygenation of arachidonic acid in settings of oxidative injury and cyclooxygenase activation, respectively. These compounds rapidly adduct to proteins via lysyl residues, which can alter protein structure/function. We examined whether pyridoxamine, which has been shown to scavenge α-ketoaldehydes formed by carbohydrate or lipid peroxidation, could also effectively protect proteins from the more reactive γ-ketoaldehydes. Pyridoxamine prevented adduction of ovalbumin and also prevented inhibition of RNase A and glutathione reductase activity by the synthetic γ-ketoaldehyde, 15-E_2-isoketal. We identified the major products of the reaction of pyridoxamine with the 15-E_2-isoketal, including a stable lactam adduct. Two lipophilic analogs of pyridoxamine, salicylamine and 5'*O*-pentylpyridoxamine, also formed lactam adducts when reacted with 15-E_2-isoketal. When we oxidized arachidonic acid in the presence of pyridoxamine or its analogs, pyridoxamine-isoketal adducts were found in significantly greater abundance than the pyridoxamine-*N*-acyl adducts formed by α-ketoaldehyde scavenging. Therefore, pyridoxamine and its analogs appear to preferentially scavenge γ-ketoaldehydes. Both pyridoxamine and its lipophilic analogs inhibited the formation of lysyl-levuglandin adducts in platelets activated *ex vivo* with arachidonic acid. The two lipophilic pyridoxamine analogs provided significant protection against H_2O_2-mediated cytotoxicity in HepG2 cells. These results demonstrate the utility of pyridoxamine and lipophilic pyridoxamine analogs to assess the potential contributions of isoketals and levuglandins in oxidant injury and inflammation and suggest their potential utility as pharmaceutical agents in these conditions.

Highly reactive γ-ketoaldehydes are formed via the cyclooxygenase pathway and by radical-catalyzed lipid peroxidation. Prostaglandin H_2, the product of the cyclooxygenase enzyme, rearranges in aqueous solution to form a number of eicosanoids, approximately 20% of which are the γ-ketoaldehydes levuglandin E_2 and D_2. Lipid peroxidation yields a series of

†This work was supported by National Institutes of Health Grants GM42056 (MERIT Award to L.J.R.), AG26119, GM15431 (to J.A.O.), DK26657, DK065138 (to B.G.H.), and a grant from the American Health Assistance Foundation. S.S.D. was supported by the Vanderbilt Diabetes Training and Research Center (DK20593). E.J.B. was supported by the NIH training grant T35-DK07383. J.A.O is the Thomas F. Frist, Sr. Professor of Medicine. B.H.G. is the Elliot V. Newman Professor of Medicine and Biochemistry.

*Address Correspondence to: Sean S. Davies, Department of Pharmacology, Vanderbilt University, 506A RRB 23rd Ave. S. Pierce Ave., Nashville, TN 27232-6602. Tel.: 615-322-5049; Fax: 615-322-3669 E-mail: sean.davies@vanderbilt.edu.

prostaglandin H_2 isomers that also rearrange to corresponding γ-ketoaldehydes, designated as isoketals (IsoK). These γ-ketoaldehydes (γKAs) react extremely rapidly with the lysyl residues of protein to form stable adducts, including a lysyl-lactam adduct and intermolecular crosslinks (1-4). Levels of γKA adducts significantly increase in pathological conditions including atherosclerosis, end-stage renal disease, and Alzheimer's Disease (5,6). Increased γKA adduct formation has also been characterized in experimental models of oxidative injury and inflammation, including carbon tetrachloride treated rats (7), hyperoxia treated mice (8), septic mice (9), and *ex vivo* activation of platelets (10). Levels of γKA adducted proteins are expected to be elevated in a wide variety of conditions previously linked to oxidative injury and inflammation (11-23). While the potent cytotoxicity of γKAs and their ability to induce protein aggregation and to disrupt enzymatic function indicate a strong pathologic potential (24-27), meaningful investigation into the extent to which formation of γKA adducts on proteins contributes to disease will require methods to selectively reduce the levels of γKA adducts *in vivo*.

One strategy for inhibiting γKA adduction to proteins is simply to reduce the formation of γKAs with antioxidants and cyclooxygenase inhibitors (NSAIDS or coxibs). However, since neither of these approaches selectively inhibits the formation of γKAs, it would not be possible to assess the pathophysiologic importance of the formation of these γKAs in settings of oxidant injury and inflammation. Therefore, we sought to develop strategies to selectively scavenge γKAs before they adduct to proteins (Figure 1). An effective scavenger would need to react significantly faster with γKAs than the γKAs react with lysyl residues of protein and would have to achieve sufficient concentrations *in vivo* to compete effectively with lysyl residues (28).

One important candidate for an effective γKA scavenger is pyridoxamine (PM), a vitamin B_6 vitamer. We previously determined that the reaction rate of γKA with PM to form pyrrole adducts was over 2000 times greater than its reaction rate with *N*-acetyllysine (29). PM can be delivered at relatively high concentration in vivo. Supplementation of drinking water with 2 g/L PM gave plasma PM concentration of 6 μM in healthy rats and more than 100 μM in streptozotocin-diabetic rats (30). PM can also scavenge a number of α-ketoaldehydes formed during glucose or lipid degradation (31,32). Therefore, we thought it would be useful to determine the relative amounts of PM products formed from both of these classes of aldehydes during lipid peroxidation.

PM is quite hydrophilic, and we have previously found that IsoK formation initially occurs in situ on membrane phospholipids (7). Therefore, modification of PM in a way that retained its high reactivity but increases its lipophilicity could enhance its effectiveness as a scavenger. We previously found that salicylamine (SA), which readily dissolves in ethyl acetate, also rapidly reacted with γKAs (29). We interpreted this finding to suggest that an aminomethyl group and an adjacent hydroxyl on an aromatic ring were the critical components for γKA scavenging. This result also suggests that converting the β-hydroxyl group at the 5'-position of PM to an ether would not interfere with γKA scavenging. Such ethers should be substantially more lipophilic than PM. We therefore examined the properties of PM and two lipophilic analogs to determine their potential usefulness as selective agents to reduce γKA protein adduct formation.

EXPERIMENTAL PROCEDURES

Materials

Unlabeled 15-E_2-IsoK, methyl ester-[12-^{3}H]-15-E_2-IsoK ([^{3}H]-MeIsoK), and [$^{13}C_3$]-15-E_2-IsoK were synthesized by the method of Amarnath *et al.*(33) [4-^{3}H] 4-hydroxy-2(E)-nonenal ([^{3}H]-HNE) was synthesized according to the published methods (34). Pyridoxamine

dihydrochloride, arachidonic acid, chicken egg ovalbumin (OVA), yeast RNA, Baker's yeast glutathione reductase, oxidized glutathione, sodium citrate, citric acid and NADPH were purchased from Sigma-Aldrich (St. Louis, MO). Pyridoxamine free base was a generous gift from BioStratum, Inc (Durham, NC). Salicylamine was purchased from Fischer Scientific USA (Pittsburgh, PA) and additional salicylamine hydrochloride was synthesized by the method of Reany et al (35) RNase A was obtained from Worthington Biochemical (Lakewood, NJ). Dazoxiben was a generous gift from Pfizer Limited (Sandwich, U.K.). Sepharose 2B was from Amersham Pharmacia Biotech (Uppsala, Sweden). Sep Pak tC18 cartridges were obtained from Waters Corp. (Milford, MA). Pronase and aminopeptidase M from porcine kidney were from Calbiochem (San Diego, CA).

Synthesis of 5′-O-Pentylpyridoxamine (PPM)

Pyridoxine was converted to 3,4′-*O*-isopropylidenepyridoxine (36), which was added to a suspension of NaH (4 g of 60% suspension in oil, 50 mmol) in THF (50 mL) under argon. The reaction mixture was refluxed for 30 m and a solution of 1-iodopentane (6 mL, 45 mmol) in THF (10 mL) and DMF (20 mL) was added over 1 h. After cooling, saturated NH_4Cl (100 mL) was added to quench the reaction and 3,4′-*O*-isopropylidene-5′-*O*-pentylpyridoxine was extracted with CH_2Cl_2 (3 × 20 mL); yield 5.1 g (70%). The pentyl derivative (8 g) was heated with 1:1 water-formic acid (32 mL) at 50 °C for 4 h. The reaction mixture was evaporated, and the residue was dissolved in ethyl acetate (75 mL), washed with 10 M $NaHCO_3$ (30 mL), and dried(37). Pure 5′-*O*-pentylpyridoxine (5.8 g) was obtained as a white solid (m.p. 114-115 °C) after purification on a column of silica using 1:2 hexane-ethyl acetate. It (2.4 g, 10 mmol) was dissolved in $CHCl_3$ (50 mL) and stirred with MnO_2 (3.6 g) for 18 h. The solid was removed by filtration, and the filtrate was concentrated and stirred with $NH_2OH.HCl$ (0.6 g) and CH_3CO_2Na (0.7 g) in ethanol to obtain 5′-*O*-pentylpyridoxal oxime; 1.6 g (65%); MS *m/z* 253 (M + 1), 235 (M $-H_2O$). The oxime (2.5 g, 10 mmol) was dissolved in acetic acid (15 mL), cooled to 10 °C in a large ice-water bath, and stirred with zinc dust (2.6 g) at 10-15 °C for 1 h and at room temperature for 1 h. Solid was removed by filtration through a bed of Celite and the filtrate was evaporated. The residue was taken in water (10 mL) and pH raised to 8.5 with 1 M NH_4OH. Water was removed, and the residue was dissolved in methanol (15 mL) and purified by flash chromatography (10-30% methanol in acetic acid) to white solid; 1.6 g (67%); m.p. 118-120 °C; MS *m/z* 239 (M + 1), 222 (M – NH_2), 151 (222 – C_5H_{11}), 136 (151 – CH_3). To determine the second order rate constant for pyrrole formation with a model γKA, 4-oxo-pentanal, 1 mM each of 4-oxo-pentanal and PPM, PM, or SA were incubated together and measurements carried out as described in (29) except that the reaction buffer was 50 mM phosphate buffer in 1:1 acetonitrile-water.

Measurement of HNE and isoketal adduction

10 mM PM, 10 mM N^{α}-acetylcysteine, and 100 μM OVA were prepared in water. OVA (0.45 mg/ml final concentration) was incubated in phosphate buffered saline (PBS) with up to 1 mM PM, 100 mM N^{α}-acetyllysine, or 1 mM N^{α}-acetylcysteine and [^{3}H]-MeIsoK (50 μM) or [^{3}H]-HNE (50 μM) in 750 μl final volume. [^{3}H]-MeIsoK was used instead of IsoK free acid because of its availability and to simplify extraction of unadducted compound into ethanol. The reaction rates of MeIsoK and IsoK do not differ significantly (unpublished observations). A solution without OVA was used as a negative control. [^{3}H]-MeIsoK was incubated for 2 hours. Because of the considerably slower reaction rate of HNE, [^{3}H]-HNE was incubated for 24 hours to achieve similar rate of adduction as with [^{3}H]-IsoK. 750 μl of ice cold ethanol was added, vortexed, and the solution centrifuged at ~14,000 × g for 15 minutes at 4 °C to pellet OVA. The supernatant was removed, and the pellet washed with another 1 ml of ice cold ethanol. The supernatant was again removed and the radioactivity remaining in the pellet determined by liquid scintillation counter. The amount of radioactivity pelleted in the absence of inhibitor

was set as 100% adduction, and the amount of pelleted radioactivity when no protein was present set at 0%.

Measurement of RNase and glutathione reductase activity

RNase activity was determined by measuring the formation of acid-soluble oligonucleotide, as described by Kalnitsky *et al*. (38), with modifications. For the assay, 100 μl of 3 μg/ml RNase in 100 mM sodium-acetate, pH 5.0 was mixed with 100 μl of 1% yeast RNA in the same buffer. After incubation at 37 °C for 5 min, the reaction was stopped by the addition of 100 μl of an ice-cold solution of 0.8% lanthanum nitrate in 18% perchloric acid. Incubation tubes were kept on ice for 5 min to ensure complete precipitation of undigested RNA and then centrifuged at 12,000 × g for 10 min. An aliquot of the supernatant (20 μl) was diluted to 1 ml with distilled water and the amount of digested (solubilized) RNA was determined by measuring absorbance at 260 nm. The activity of RNase A incubated alone at 37 °C was monitored separately and used as the reference for each incubation time. This reference activity did not change significantly over the course of incubation.

Glutathione reductase (GR) activity was determined by measuring the initial rate of NADPH consumption (39). The mixture of 1 mM GSSG and 0.3 mM NADPH was incubated in 200 mM Tris-HCl buffer, pH 7.5 at 37 °C in a temperature-controlled spectrophotometer cell equipped with magnetic mixer. After the equilibration of the temperature and baseline stabilization, GR was added to the spectrophotometric cell to make 0.06 U/ml GR. The activity was assayed at 37 °C by monitoring the absorbance at 340 nm for 1 min at 0.1 min intervals. The rate of NADPH consumption was calculated using Carry 100 Bio UV-Visible spectrophotometer software.

Identification of γKA-PM adducts

Synthetic 15-E_2-IsoK or [$^{13}C_3$]-15-E_2-IsoK (250 μM final concentration) was incubated with 1 mM PM overnight at 37 °C in triethylamine acetate buffer (pH 8.0). Separate experiments were also carried out in PBS. Additional control reactions with IsoK or PM alone were also carried out under identical conditions. The resulting products were analyzed by mass spectrometry using a ThermoFinnigan (San Jose, CA) TSQ Quantum triple quadrupole mass spectrometer equipped with a standard electrospray ionization source. Nitrogen was used for both the sheath and auxiliary gas. The mass spectrometer was operated in the positive ion mode and the electrospray needle potential maintained at 4000 V. The ion transfer tube was operated at 35V and 210 °C. The tube lens voltage was set to 90 V. Source CID was 5V. Full scan spectra were acquired from m/z 450 to 550 over 1 second. Xcalibur™ Software, version 1.3, from ThermoFinnigan was used to control all instruments and to process the data. Novel ions present only in the reaction with both IsoK and PM were subjected to collision-induced disassociation at a collision energy of 30 eV followed by product ion scan.

Quantification of adducts formed during free radical catalyzed oxidation of arachidonic acid

Arachidonic acid (10 mM) was oxidized in 5 ml PBS using iron/ADP/ascorbic acid as previously described (40) for two hours, except that we added 20% isopropyl alcohol to improve solubility of oxidation productions. To minimize potential effects of iron chelation by pyridoxamine or its analogs, the analogs and lysine were not added to the mixture during this initial period of lipid peroxide formation. After two hours, a solution containing 2 mM final concentration of lysine and 100 μM final concentration of appropriate scavenger was added to the reaction, which was then further incubated for 22 hours. [$^{13}C_6$ $^{15}N_2$]-lysyl-IsoK-lactam and [$_2H_4$]-15$_{2t}$-isoprostane were added as internal standards. Lysine and PM or PM analog adducts were analyzed by LC/MS/MS using high through-put C18 column (Magic Bullet C18 column 3A, Michrom BioResources, Auburn, CA) with the gradient programmed from 100% solvent A (5 mM ammonium acetate with 0.1% acetic acid) to 100% Solvent B

(acetonitrile/methanol 95:5) from 0.5 minutes to 3.0 minutes and then continuing at 100% B for an additional 1.5 minutes. The column volume for this column is 25 ul and the flow rate was 190 μl/min (7.6 column volumes/min). Eluant was coupled directly to the mass spectrometer operated in selective reaction monitoring (SRM) positive ion mode. For all reactions, SRM was performed at *m/z* 479.3 →84.1, 30 eV (lysyl-IsoK-lactam); m/z 487.3→84.1, 30eV ([$^{13}C_6$ $^{15}N_2$]lysyl-IsoK-lactam. Additionally, the appropriate SRM for adducts of the particular PM analog was performed as shown in Table 1. In summary, precursor masses for the *N*-pentanedioyl and *N*-hexanoyl (41), as well as the isoketal-lactam adducts were chosen based on those formed with PM so that 114, 98, and 332 daltons, respectively were added to the appropriate PM analog [M+H^+] mass. Product ion masses were calculated as -17 daltons (deamidation fragmentation) from appropriate PM analog [M+H^+] mass. The collisional energy was 30 eV for all transitions. The ratio of the area of individual peak to the area of [$^{13}C_6$ $^{15}N_2$] lysyl-IsoK-lactam peak was used for quantification.

For analysis of F_2-isoprostanes (F_2-IsoP), the mass spectrometer was set to selective reaction monitoring in negative ion mode for *m/z* 353.3→309.1, 30 eV (F_2-IsoP) and *m/z* 357.3→313.1,30 eV ([$^2H_4$]-8-epi-PGF_2).

Measurement of cyclooxygenase products in platelets

Human blood was obtained following a protocol approved by the Institutional Review Board of Vanderbilt University. Washed human platelets were isolated as described previously (42, 43). The eluted platelets were counted with a Coulter counter and diluted with buffer (8.3 mM sodium phosphate pH 7.5, 0.109 M NaCl, 5.5 mM glucose) to a final count of 600,000 platelets/μl. Washed platelets were then pre-incubated with the thromboxane synthase inhibitor, dazoxiben (final concentration of 10 μM), and either vehicle or PM analogs (final concentration of 100 μM or 1mM) for 30 min at room temperature. At this time, the platelets were activated by adding arachidonic acid (20 μM final concentration) and incubated at room temperature for 2 hours. After incubation, platelets were pelleted at 2,000 × g for 10 min at 4 °C. After centrifugation, the lysyl-levuglandin- lactam adduct was isolated from a proteolytic digest of the pelleted proteins and analyzed by high-performance liquid chromatography coupled to tandem mass spectrometry (LC/MS/MS) as described previously (1,10,44). Levels of prostaglandin E_2 (PGE_2) in the platelet supernatant were analyzed by GC/MS as previously described (2).

H_2O_2 induced cytotoxicity in HepG2 cells

Confluent HepG2 cells were trypsinized and resuspended in Dulbecco's Modified Eagle's Medium (Mediatech, Inc. Herndon, VA) containing 10% serum (Hyclone, Logan, UT) and penicillin, streptomycin, and amphocetrin (DMEM) at 2 × 10^5 cells/ml and 100 μl of this solution added to each well of multiple CulturPlate TC-96 well plates (Perkin-Elmer, Boston, MA) and the cells allowed to adhere for 4 hours. Cells were then pretreated with the appropriate PM analog for 45 minutes and then eight replicate wells were treated with each concentration of H_2O_2 for 24 hours. This time point was chosen because preliminary experiments showed that most of the cytotoxicity occurred within the first four hours of exposure to oxidation. Therefore, if PM analogs only slowed or delayed the onset of cytotoxicity induced by oxidation, the measurements at 24 hours would still likely capture the full extent of cytotoxicity induced by H_2O_2 under these conditions. The viability of cells were quantified by measuring ATP levels (45) with the ATPlite luminescence ATP detection assay system (Perkin-Elmer) using a Packard Lumicount luminescent microplate reader (Global Medical Instrumentation, Ramsey, MN). The percent viability of each well was calculated by dividing the individual well value by the average value of the replicate wells untreated with H_2O_2 in the same plate. Statistical analysis was performed using GraphPad Prism 4.0 (GraphPad Software, Inc. San Diego, CA).

RESULTS

Pyridoxamine protects proteins from adduction by γKAs

We previously determined that the reaction of pyridoxamine with a model γKA, 4-oxo-pentanal, is more than 2,000 times faster than that of N^{α}-acetyllysine with 4-oxopentanal (29). To test whether PM would prevent the adduction of γKAs to protein, we incubated a model protein, ovalbumin (OVA), with 50 μM of the methyl ester of 15-E_2-IsoK containing tracer amounts of radiolabel ([^{3}H]-MeIsoK) in the presence of various concentrations of PM or N^{α}-acetyllysine. The extent of [^{3}H]-MeIsoK adduction was determined as the amount of radioactivity present in the ethanol-precipitated protein. PM dose-dependently inhibited the adduction by [^{3}H]-MeIsoK to OVA (IC_{50} 88 μM), with 1 mM PM sufficient to completely prevent [^{3}H]-MeIsoK adduction (Figure 2A). In contrast, coincubation of OVA with even 100 mM N^{α}-acetyllysine still allowed 38% [^{3}H]-MeIsoK binding. These results indicate that PM, as expected, is a far better scavenger of γKAs than N^{α}-acetyllysine and can also compete effectively with protein lysyl residues for IsoK. Interestingly, 0.1 mM and 1 mM N^{α}-acetyllysine actually increased the amount of [^{3}H]-MeIsoK binding over that with vehicle alone. Presumably, this increase results from secondary reactions of N^{α}-acetyl-lysyl-pyrrole adducts to form crosslinks with OVA. Cysteine residues from OVA would be expected to more freely participate in crosslinking reactions with the more mobile N^{α}-acetyl-lysyl-pyrroles than with intramolecular lysyl-pyrroles.

HNE is a major product of lipid peroxidation that also adducts to proteins, but primarily via Michael addition reactions with cysteine residues. No HNE-PM adduct has been identified with PM (29,32), yet PM prevents the formation of HNE-lysine adducts during oxidation of arachidonic acid (32). Because PM might have potentially inactivated HNE by formation of an intermediate that was simply too unstable for analysis, we tested the effect of PM on [^{3}H]-HNE adduction to OVA. PM did not significantly decrease the amount of [^{3}H]-HNE binding to OVA even at 1 mM (Figure 2B). In contrast, N^{α}-acetyl-cysteine, an excellent direct scavenger of HNE, effectively protected OVA from adduction by [^{3}H]-HNE (IC_{50} 129 μM).

Pyridoxamine protects enzymes from inhibition by γKAs

The effective elimination of γKA adduction to OVA by PM suggested that PM should also protect enzymatic activity from inhibition by γKAs. We chose RNase A as a model enzyme because it features a catalytically important lysine residue. Preincubation of RNase A with increasing concentrations of IsoK for two hours resulted in dose-dependent inhibition of activity (IC_{50} 38 μM) (Figure 3A). Addition of 200 μM IsoK led to 50% inhibition in less than 12 minutes, with complete inhibition achieved somewhere between one and two hours (Figure 3B). Preincubation of RNase A with 500 μM PM completely protected RNase activity from inhibition by 200 μM IsoK at all time points. Lower concentrations of PM still partially protected RNase A activity (not shown). Similarly, PM also protected another model enzyme, glutathione reductase, from inhibition by IsoK (Figure 3C).

Pyridoxamine reacts with IsoK to form stable PM-pyrrole adducts

In order to compare the ability of pyridoxamine to scavenge various α and γ-ketoaldydes formed during lipid peroxidation, we determined the major products formed by the reaction of 15-E_2-IsoK with PM. Our expectations of potential products were based on our previous studies of the products of the reaction of γKAs with lysine, where the major stable products are the oxidized pyrrole species, lactam and hydroxylactam adducts (1). We incubated 1 mM PM with 250 μM IsoK or [$^{13}C_3$]-IsoK overnight at 37 °C and analyzed the resulting products. Previously, the reaction of PM with glyoxal was shown to cause a shift in the absorbance maxima of PM from 324 nm to 282 nm (31). In contrast, we found that the reaction of IsoK with PM did not cause significant changes in the absorption spectrum of PM (Figure 4A). This result suggests

that the 3-hydroxypyridine moiety is preserved during the reaction, as would be expected for pyrrole formation and subsequent oxidation.

To further characterize the product of the IsoK reaction with PM, we analyzed the products by electrospray ionization mass spectrometry operating in the positive ion mode. Limited mass scanning of the reaction products revealed three major species with *m/z* 467, *m/z* 485, and *m/z* 501 (Figure 4B). These masses are consistent with PM-IsoK-anhydro-pyrrole, PM-IsoK-pyrrole, and PM-IsoK-lactam adducts, respectively. Analysis of the reaction products of [$^{13}C_3$]-IsoK with PM showed ions at *m/z* 470, *m/z* 488, and *m/z* 504, consistent with the heavy isotope species of these same products (data not shown)

The lysyl-IsoK-lactam adduct is very stable, suggesting that the putative PM-IsoK-lactam would also be a stable product useful for analysis. We therefore chose to further characterize the putative PM-IsoK-lactam species. Collision induced disassociation (CID) of the *m/z* 501 ion gave prominent ions at *m/z* 152, *m/z* 314, *m/z* 332, *m/z* 465, and *m/z* 483 (Figure 5C). The CID spectrum of the PM-[$^{13}C_3$]-IsoK product *m/z* 504 ion gave rise to product ions with *m/z* 152, *m/z* 317, *m/z* 335, and *m/z* 486 (data not shown). Our interpretation of the CID spectrum is shown in Figure 4C and is consistent with PM-IsoK-lactam. Fragmentation of PM and many PM adducts give rise to an *m/z* 152 ion, consistent with the deamidation of PM by fragmentation of the β-amine (32, 41). Fragmentation of this same bond with loss of one water molecule also gives rise to the *m/z* 332 ion, (*m/z* 335 for the PM-[$^{13}C_3$]-IsoK product). Previously, we showed that fragmentation of the analogous bond in the lysyl-IsoK-lactam adduct results in a *m/z* 332 product ion as one of the most prominent species (1). We interpret the *m/z* 314 ion to result from the loss of a second water molecule from this fragmentation product. The *m/z* 483 and *m/z* 465 likely arise from the loss of one and two water molecules, respectively, from the parent molecular ion.

Synthesis of 5'-O-pentylpyridoxamine

PM is strongly hydrophilic, but isoketal formation is expected to primarily occur in phospholipid membranes. Therefore, lipophilic analogs of PM may be more useful scavengers of endogenously formed isoketals. Salicylamine, like PM, includes adjacent methylamine and hydroxyl substituents on an aromatic ring, and reacts only slightly slower than PM with γ-ketoaldehydes in PBS (29), but is much more lipophilic because there is no pyridine ring nitrogen. To retain all of the structural determinants of PM, but to increase lipophilicity, we also modified PM by converting the 5'-hydroxyl group to a pentyl ether group to form 5'-*O*-pentylpyridoxamine (Figure 5). Unlike PM, both 5'-*O*-pentylpyridoxamine (PPM) and salicylamine (SA) partition into ethyl acetate from water as expected for lipophilic compounds. We then determined the second order rate constant for pyrrole formation by the three compounds when reacted with a model γKA, 4-oxo-pentanal. A 1:1 acetonitrile/phosphate buffer solution has been proposed as a reasonable model of the low dielectric microenvironment of cellular membranes (46). In 1:1 acetonitrile/phosphate buffer, the second order rate constant for SA (2.17±0.26 L/s*mol) was 1.2 times faster than that of PM (1.84 ±0.17) or PPM (1.87±0.08). When the two lipophilic PM analogs were reacted with 15-E_2-isoketal, both formed precursor and product ions with the expected m/z for IsoK-lactam adducts (data not shown).

IsoK-lactam adduct is a major product of PM analog scavenging during oxidation of arachidonic acid

Scavenging of αKAs and other lipid and carbohydrate degradation products (30-32,41,47, 48), as well as chelation of redox active metals (49,50) have previously been demonstrated to contribute to the protective effects of PM during lipid peroxidation. However, our previous finding of greater reactivity of PM with γKAs suggested that where the ratio of PM was limiting,

PM scavenging of lipoxidation aldehydes would be primarily directed towards γKAs (29). To test this possibility, we incubated 10 mM arachidonic acid with an oxidizing solution of iron/ADP/ascorbate for 2 hours to initially form lipid peroxides, and then incubated this reaction mixture for an additional 22 hours in the presence of 1 mM lysine and 100 μM of PM or its lipophilic analogs, after which we measured the two most abundant putative α-ketoaldehyde adducts, *N*-pentanedioyl and *N*-hexanoyl, along with the IsoK-lactam adduct using LC/MS/MS with [$^{13}C_6$ $^{15}N_2$]-lysyl-IsoK-lactam as an internal standard (Figure 6).

Iron mediated oxidation of arachidonic acid in the presence of lysine and vehicle (PBS) resulted in the robust formation of lysyl-IsoK-lactam adduct (Figure 6A). Coincubation with 100 μM of PM, PPM, or SA reduced the amount of lysyl-IsoK-lysine adduct by 81%, 71%, and 71%, respectively ($p \leq 0.01$). The decrease in lysyl-IsoK-lactam formation by PM analogs was not accompanied by a reduction in F_2-isoprostane levels (Figure 6B), a non-reactive product of the lipid peroxidation pathway. Therefore, although PM analogs have the potential to reduce lipid peroxidation by iron chelation, a reduction of lipid peroxidation and thus isoprostane and IsoK formation is not likely to be the cause of the decreased lysyl adduction under these experimental conditions.

Consistent with scavenging being the primary mechanism for inhibition of lysyl-IsoK-lactam formation, coincubation with PM was accompanied by the formation of PM-IsoK-lactam adduct. In the reactions with lysine only, 136 ng of lysyl-IsoK-lactam formed. In contrast, in the reactions coincubated with PM only 31 ng of lysyl-IsoK-lactam formed, while the signal for the PM-IsoK-lactam was 2.4-fold higher than that of the lysyl-IsoK-lactam in this reaction, so that we estimate that 74 ng of PM-IsoK-lactam formed. The potential differences in ionization and fragmentation efficiency of PM versus lysine adduct makes quantification of their relative concentrations using a single internal standard somewhat inexact; nevertheless, a significant proportion of the IsoK appears to be diverted from reacting with lysine by reacting with PM.

Deamidation fragmentation during LC/MS/MS of the PM-IsoK-lactam, PM-*N*-pentanediolyl and PM-*N*-hexanoyl adducts yields the same product ion at *m/z* 152 (32,41), so that monitoring the ion current for this product ion is likely to be a relatively accurate measure of the abundance of each precursor. PPM and SA also undergo similar deamidation fragmentation during LC/MS/MS to yield product ions of *m/z* 222 and 107, respectively (data not shown). To compare the relative yield of α-ketoaldehyde versus γ-ketoaldehyde products scavenged by these PM analogs during arachidonic acid oxidation, we performed SRM for the expected precursor mass for the IsoK-lactam, *N*-pentadioyl, and *N*-hexanoyl adduct of each PM analog with transition to the appropriate product ion (Table 1), integrated the relative peak area for each product, and then normalized these values to the average IsoK-lactam value. For each PM analog, the γKA product, IsoK-lactam, was formed in far greater abundance than the putative α-ketoaldehyde products, *N*-pentanedioyl and *N*-hexanoyl (Figure 6C).

PM protects against γKAs formed endogenously in cells

While our results suggest that PM analogs are effective γ-KA scavengers in vitro, the intracellular milieu contains an undefined amount of lysyl residues and microdomains that may prevent the effective scavenging of γKAs formed endogenously. We have previously demonstrated that levuglandin adducts form in stimulated platelets after activation with arachidonic acid, and that levuglandin adducts levels can be further increased by pretreatment of platelets with dazoxiben, a thromboxane synthase inhibitor (10). We therefore preincubated platelets with dazoxiben and 100 μM or 1 mM PM analog and measured the amount of lysyl-γKA-lactam adduct formed. Lysyl-levuglandin-lactam adduct was reduced by 29%, 31%, and 64% by 100 μM PM, PPM or SA, respectively ($p < 0.05$) and by 70% 78%, and 86%, by 1 mM PM, PPM, or SA, respectively ($p<0.001$). To exclude the possibility of direct inhibition

of cyclooxygenase activity by PM analogs, we measured the effect of the PM analogs on the major product of PGH_2 synthesis in dazoxiben-inhibited platelets, PGE_2. In contrast to inhibiting lysyl-levuglandin-lactam formation, PM analogs did not inhibit formation of PGE_2 (Figure 7B), and in fact SA slightly, but significantly increased PGE_2 formation. Therefore, the reduction of protein adducts by PM analogs is most likely due to direct scavenging of levuglandin and not by inhibition of cyclooxygenase activity. The slight increase in PGE_2 levels in platelets incubated with SA could be a result of SA protecting cyclooxygenase from modification by levuglandin, as we have previously shown that cyclooxgenase becomes modified by levuglandin as a consequence of its synthesis of PGH_2 (51).

PM analogs protect against H_2O_2 mediated cytotoxicity

To examine whether blocking protein-isoketal adduct formation during oxidant stress had a significant biological impact, we examined whether lipophilic PM analogs would provide protection against oxidant-induced cytotoxicity. Isoketals are one of the most cytotoxic products of lipid peroxidation (24) and hydrogen peroxide (H_2O_2) is a well-studied inducer of the isoprostane pathway of lipid peroxidation (52-57) and cytotoxicity (58,59). We performed a preliminary dose curve in cultured HepG2 cells to determine the maximal concentrations of each PM analogs that would not induce cytotoxicity. No significant loss of HepG2 cell viability was seen at 2 mM PM, 1 mM SA, or 1 mM PPM (data not shown). To determine the effect of the PM analogs on H_2O_2 induced toxicity, we preincubated HepG2 cells with either vehicle only (DMEM), 2 mM PM, 0.5 mM PPM, or 0.5 mM SA, for 45 minutes and then treated the cells with either 0, 25, 75, 125, 250, 500, or 750 uM H_2O_2 for 24 hours. H_2O_2 dose-dependently reduced the viability of vehicle only pretreated cells (estimated LC_{50} 54 μM), with essentially complete toxicity induced by 125 μM H_2O_2 (Figure 8). While H_2O_2 also dose-dependently reduced the viability of SA, PPM, and PM pretreated cells ($p < 0.0001$, 2-way ANOVA for vehicle vs individual PM analogs), preincubation with the two lipophilic PM analogs caused a significant rightward shift in the concentration of H_2O_2 required to induce cytotoxicity, (estimated LC_{50} of 221 μM, $p < 0.0001$, 2-way ANOVA, vehicle vs SA pretreatment; and estimated LC_{50} 124μM, $p < 0.0015$; 2-way ANOVA, vehicle vs PPM pretreatment). In contrast, preincubation with even 2 mM PM did not significantly enhance viability after exposure to H_2O_2 (estimated LC_{50} 43 μM, $p = 0.333$, 2-way ANOVA, vehicle vs PM treatment.) The ability of lipophilic PM analogs to significantly protect against H_2O_2 induced cytotoxicity suggests that esterifed-IsoKs are an important mediator of H_2O_2 cytotoxicity.

DISCUSSION

Previous work showed that the levels of IsoK and levuglandin protein adducts increase in a number of pathological conditions (5-9)(6), suggesting that these γKAs might contribute to the pathogenesis of disease. To investigate the contribution of these adducts to disease, we sought effective methods to prevent formation of these protein adducts. One of the most promising and selective strategies might be to scavenge these γKA with amine containing compounds that are more reactive than lysyl groups. Previous observations suggested that PM was a good candidate for a γKA scavenger because it reacts with γKAs about 2,000 times faster than does lysine (29). Our present study showed that PM significantly inhibited the formation of lysyl-IsoK adducts when coincubated with excess lysine and oxidized arachidonic acid. PM also protected proteins and their enzymatic activity against adduction by IsoKs and levuglandins when added in vitro. Importantly, PM provided protection to platelet proteins against adduction by levuglandin formed endogenously during ex vivo activation by arachidonic acid. Thus PM appears to be a very useful agent to scavenge the levuglandins formed by cyclooxygenase or non-esterified IsoKs formed by free radical oxidation of arachidonic acid and could be used to investigate the contribution of levuglandins in cell culture models of cyclooxygenase-mediated events.

While PM is useful to scavenge the non-esterified forms of γKA, its hydrophilicity may limit its efficacy under conditions where oxidation occurs with esterified arachidonic acid. We hypothesized that the basic structure of PM could be modified to be more lipophilic while still retaining its high reactivity for γKAs. SA was previously shown to also rapidly react with γKAs, suggesting that the critical components for γKA scavenging were an aminomethyl group and an adjacent hydroxyl on an aromatic ring. We reasoned, therefore, that converting the β-hydroxyl group at the 5'-position of PM to a pentyl ether to form PPM would not interfere with γKA scavenging, but would increase lipophilicity. The reaction rate of PPM with the model γKA, 4-oxo-pentanal, was identical to PM and the reaction rate of SA was slightly faster when 50% acetonitrile was used as the reaction solvent. When the PM analogs were added to a 10-fold greater concentration of lysine and then incubated with oxidized arachidonic acid, all three analogs inhibited the formation of lysyl-IsoK-lactam adduct about equally well. These results are consistent with our postulated mechanism for PM as a γKA scavenger and demonstrate that the basic structure of PM can be readily modified to form more lipophilic analogs that retain the rapid reactivity required for γKA scavenging.

PM scavenges α-ketoaldehydes formed from carbohydrate and lipid degradation. We have previously reported 4-oxo-pentanal reacted about 190 times faster with PM than a model α-ketoaldehyde, methylglyoxal, and that PM does not react to a significant extent with HNE (29). Therefore, we would expect abundant IsoK adduct formation along with the formation of *N*-acyl adducts of PM when arachidonic acid was oxidized in the presence of PM or its lipophilic analogs. However, studies by Metz et al examining the products formed by non-catalyzed oxidation of arachidonic acid in the presence of PM did not report finding a product corresponding to an IsoK adduct (41). We therefore characterized the PM and PM analog adducts formed by reaction with 15-E_2-IsoK, and then examined whether PM or its lipophilic analogs formed this PM analog-IsoK-lactam adduct during iron-catalyzed arachidonic acid oxidation using these analytical methods to determine its abundance relative to *N*-acyl adducts. Using our experimental and analytical methods, we found that PM- and PM analog-IsoK-lactam adducts were formed in far greater abundance than *N*-acyl-adducts. These results suggest that PM and its analogs strongly favor scavenging γKAs, so that at least some of the beneficial effects seen with PM supplementation in diabetic animals (30,41,47) may derive from the inhibition of protein-γKA adduct formation.

The mechanism we postulated for the reactivity of PM with γKAs (29), also rationalizes the selectivity of PM and its analogs towards γKAs. While all aldehydes should react with PM at approximately the same rate to form the initial, reversible hemiaminal adduct, only the hemiaminal formed by γKAs can go on to attack the ketone moiety of the γKA and form an irreversible pyrrole adduct, thus driving the reaction rapidly forward. The presence of the phenolic hydroxyl group likely accelerates pyrrole formation by protonating the ketone moiety of the γKA and holding it in place for attack by the hemiaminal. The α-ketoaldehyde hemiaminal can not form a pyrrole, but as proposed by Metz et al (37), the phenolic hydroxyl group may still increase the reactivity of the amine by attacking the ketone to transiently form a seven membered ring that would then fragment to form an amide. Although this reaction for α-ketoaldehydes would not be nearly as favored as pyrrole formation for γKAs, it would still be favored over the reaction of the α-ketoaldehyde with lysyl groups.

The potential greater utility of lipophilic PM analogs over PM itself was borne out in a cellular model of oxidant injury. IsoKs are highly cytotoxic, so that we anticipated that they might make important contributions to cytotoxicity induced by reactive oxygen species. Treatment with H_2O_2 can induce cytotoxicity both by apoptosis and by necrosis, depending on its concentration (60,61). Treatment with H_2O_2 induces the formation of the mitochondrial permeability transition pore and the collapse of mitochondrial membrane potential, thereby triggering apoptosis (59,62-64). Phospholipid-bound IsoKs would be well positioned to adduct

to mitochondrial proteins regulating pore formation and membrane potential. We therefore utilized PM analogs to examine the potential role of IsoKs in HepG2 cells exposed to H_2O_2. We found that the two lipophilic PM analogs provided significant protection, such that substantial viability was seen at H_2O_2 concentrations that are normally completely cytotoxic. In contrast, even a four-fold greater concentration of hydrophilic PM did not provide any significant protection against H_2O_2-induced cytotoxicity. The lack of efficacy of PM in this cellular system suggests that PM does not reach the sites of IsoK adduction critical for cytotoxicity, either because it does not enter cells as readily as lipophilic PM analogs or does not partition to the same extent as lipophilic PM analogs into the membranes which are the principle sites of IsoK formation. Further studies investigating the effect of lipophilic PM analogs on known signaling pathways leading to cell death should yield important information about the mechanisms underlying IsoK-induced cytotoxicity. While the present studies do not rule out additional mechanisms of cytoprotection by PM analogs besides that of IsoK scavenging, the lack of efficacy of PM does suggest that metal chelation is not an important mechanism of protection from H_2O_2 under these conditions, because all three PM analogs chelate metals equally well.

While the effects of lipophilic PM analogs on HepG2 cells suggest their potential as therapeutic agents, the utility of these compounds will be dependent on whether effective concentrations can be delivered in vivo without toxicity. The concentrations of lipophilic PM analogs used in the HepG2 cell study were relatively high (500 μM), but we did not determine the minimum concentration required for cytoprotection. Approximately 100 μM plasma concentrations of PM were reported in diabetic rats given 1 g/L PM in their drinking water (30), so that it may be possible to deliver PM analogs at relatively high concentrations in vivo.

In summary, we have found that PM is an effective scavenger of non-esterified γKAs such as levuglandins and the free fatty acid form of IsoK. Modifications of PM that preserve the core phenolic amine structure, but enhance lipophilicity, retain the rapid reactivity and selectivity for γKAs, and enhance efficacy in conditions where esterified IsoKs are likely to form. The efficacy of lipophilic PM analogs against H_2O_2-induced cytotoxicity suggest a role for esterified IsoK in this model of cytotoxicity and provide the rationale for future studies to examine their potential therapeutic effects in conditions linked to oxidative injury and cyclooxygenase activation.

Acknowledgements

We thank the excellent technical assistance of Tamjeed Ahmed, Taneem Ahmin, Chris Bodine, Yao Luo, Tina Materson, Elizabeth Shipp, and Parvin Todd.

References

1. Brame CJ, Salomon RG, Morrow JD, Roberts LJ 2nd. Identification of extremely reactive gamma-ketoaldehydes (isolevuglandins) as products of the isoprostane pathway and characterization of their lysyl protein adducts. J Biol Chem 1999;274:13139–46. [PubMed: 10224068]
2. Boutaud O, Brame CJ, Salomon RG, Roberts LJ 2nd, Oates JA. Characterization of the lysyl adducts formed from prostaglandin H2 via the levuglandin pathway. Biochemistry 1999;38:9389–96. [PubMed: 10413514]
3. Iyer RS, Ghosh S, Salomon RG. Levuglandin E2 crosslinks proteins. Prostaglandins 1989;37:471–80. [PubMed: 2762557]
4. Iyer RS, Kobierski ME, Salomon RG. Generation of Pyrroles in the Reaction of Levuglandin E2 with Proteins. J Org Chem 1994;59:6038–6043.
5. Salomon RG, Batyreva E, Kaur K, Sprecher DL, Schreiber MJ, Crabb JW, Penn MS, DiCorletoe AM, Hazen SL, Podrez EA. Isolevuglandin-protein adducts in humans: products of free radical- induced

lipid oxidation through the isoprostane pathway. Biochim Biophys Acta 2000;1485:225–35. [PubMed: 10832102]

6. Zagol-Ikapitte I, Masterson TS, Amarnath V, Montine TJ, Andreasson KI, Boutaud O, Oates JA. Prostaglandin H(2)-derived adducts of proteins correlate with Alzheimer's disease severity. J Neurochem 2005;94:1140–5. [PubMed: 15992375]
7. Brame CJ, Boutaud O, Davies SS, Yang T, Oates JA, Roden D, Roberts LJ 2nd. Modification of proteins by isoketal-containing oxidized phospholipids. J Biol Chem 2004;279:13447–51. [PubMed: 14715668]
8. Davies SS, Talati M, Wang X, Mernaugh RL, Amarnath V, Fessel J, Meyrick BO, Sheller J, Roberts LJ 2nd. Localization of isoketal adducts in vivo using a single-chain antibody. Free Radic Biol Med 2004;36:1163–74. [PubMed: 15082070]
9. Poliakov E, Brennan ML, Macpherson J, Zhang R, Sha W, Narine L, Salomon RG, Hazen SL. Isolevuglandins, a novel class of isoprostenoid derivatives, function as integrated sensors of oxidant stress and are generated by myeloperoxidase in vivo. Faseb J 2003;17:2209–20. [PubMed: 14656983]
10. Boutaud O, Li J, Zagol I, Shipp EA, Davies SS, Roberts LJ 2nd, Oates JA. Levuglandinyl adducts of proteins are formed via a prostaglandin H2 synthase-dependent pathway after platelet activation. J Biol Chem 2003;278:16926–8. [PubMed: 12637576]
11. Montine TJ, Markesbery WR, Morrow JD, Roberts LJ. Cerebrospinal fluid F2-isoprostane levels are increased in Alzheimer's disease. Ann Neurol 1998;44:410–413. [PubMed: 9749613]
12. Palmer AM, Gopaul N, Dhir S, Thomas CR, Poston L, Tribe RM. Endothelial dysfunction in streptozotocin-diabetic rats is not reversed by dietary probucol or simvastatin supplementation. Diabetologia 1998;41:157–64. [PubMed: 9498648]
13. Palmer AM, Thomas CR, Gopaul N, Dhir S, Anggard EE, Poston L, Tribe RM. Dietary antioxidant supplementation reduces lipid peroxidation but impairs vascular function in small mesenteric arteries of the streptozotocin-diabetic rat. Diabetologia 1998;41:148–56. [PubMed: 9498647]
14. Montero A, Munger KA, Khan RZ, Valdivielso JM, Morrow JD, Guasch A, Ziyadeh FN, Badr KF. F(2)-isoprostanes mediate high glucose-induced TGF-beta synthesis and glomerular proteinuria in experimental type I diabetes. Kidney Int 2000;58:1963–72. [PubMed: 11044216]
15. Dworski R, Murray JJ, Roberts LJ 2nd, Oates JA, Morrow JD, Fisher L, Sheller JR. Allergen-induced synthesis of F(2)-isoprostanes in atopic asthmatics. Evidence for oxidant stress. Am J Respir Crit Care Med 1999;160:1947–51. [PubMed: 10588611]
16. Dworski R, Roberts LJ 2nd, Murray JJ, Morrow JD, Hartert TV, Sheller JR. Assessment of oxidant stress in allergic asthma by measurement of the major urinary metabolite of F2-isoprostane, 15-F2t-IsoP (8-iso- PGF2alpha). Clin Exp Allergy 2001;31:387–90. [PubMed: 11260149]
17. Montine TJ, Beal MF, Robertson D, Cudkowicz ME, Biaggioni I, O'Donnell H, Zackert WE, Roberts LJ, Morrow JD. Cerebrospinal fluid F2-isoprostanes are elevated in Huntington's disease. Neurology 1999;52:1104–1105. [PubMed: 10102447]
18. Voutilainen S, Morrow JD, Roberts LJ 2nd, Alfthan G, Alho H, Nyyssonen K, Salonen JT. Enhanced in vivo lipid peroxidation at elevated plasma total homocysteine levels. Arterioscler Thromb Vasc Biol 1999;19:1263–6. [PubMed: 10323778]
19. Pratico D, Barry OP, Lawson JA, Adiyaman M, Hwang SW, Khanapure SP, Iuliano L, Rokach J, FitzGerald GA. IPF2alpha-I: an index of lipid peroxidation in humans. Proc Natl Acad Sci U S A 1998;95:3449–54. [PubMed: 9520386]
20. Reilly M, Delanty N, Lawson JA, FitzGerald GA. Modulation of oxidant stress in vivo in chronic cigarette smokers. Circulation 1996;94:19–25. [PubMed: 8964113]
21. Laight DW, Desai KM, Gopaul NK, Anggard EE, Carrier MJ. F2-isoprostane evidence of oxidant stress in the insulin resistant, obese Zucker rat: effects of vitamin E. Eur J Pharmacol 1999;377:89–92. [PubMed: 10448931]
22. Stojiljkovic MP, Lopes HF, Zhang D, Morrow JD, Goodfriend TL, Egan BM. Increasing plasma fatty acids elevates F2-isoprostanes in humans: implications for the cardiovascular risk factor cluster. J Hypertens 2002;20:1215–21. [PubMed: 12023694]
23. Roberts CK, Vaziri ND, Barnard RJ. Effect of diet and exercise intervention on blood pressure, insulin, oxidative stress, and nitric oxide availability. Circulation 2002;106:2530–2. [PubMed: 12427646]

24. Davies SS, Amarnath V, Montine KS, Bernoud-Hubac N, Boutaud O, Montine TJ, Roberts LJ 2nd. Effects of reactive gamma-ketoaldehydes formed by the isoprostane pathway (isoketals) and cyclooxygenase pathway (levuglandins) on proteasome function. Faseb J 2002;16:715–7. [PubMed: 11978738]
25. Boutaud O, Ou JJ, Chaurand P, Caprioli RM, Montine TJ, Oates JA. Prostaglandin H2 (PGH2) accelerates formation of amyloid beta1-42 oligomers. J Neurochem 2002;82:1003–6. [PubMed: 12358806]
26. Murthi KK, Salomon RG, Sternlicht H. Levuglandin E2 inhibits mitosis and microtubule assembly. Prostaglandins 1990;39:611–22. [PubMed: 2115185]
27. Schmidley JW, Dadson J, Iyer RS, Salomon RG. Brain tissue injury and blood-brain barrier opening induced by injection of LGE2 or PGE2. Prostaglandins Leukot Essent Fatty Acids 1992;47:105–10. [PubMed: 1461920]
28. Metz TO, Alderson NL, Thorpe SR, Baynes JW. Pyridoxamine, an inhibitor of advanced glycation and lipoxidation reactions: a novel therapy for treatment of diabetic complications. Arch Biochem Biophys 2003;419:41–9. [PubMed: 14568007]
29. Amarnath V, Amarnath K, Amarnath K, Davies S, Roberts LJ II. Pyridoxamine: An Extremely Potent Scavenger of 1,4-Dicarbonyls. Chem Res Tox 2004;17:410–415.
30. Degenhardt TP, Alderson NL, Arrington DD, Beattie RJ, Basgen JM, Steffes MW, Thorpe SR, Baynes JW. Pyridoxamine inhibits early renal disease and dyslipidemia in the streptozotocin-diabetic rat. Kidney Int 2002;61:939–50. [PubMed: 11849448]
31. Voziyan PA, Metz TO, Baynes JW, Hudson BG. A post-Amadori inhibitor pyridoxamine also inhibits chemical modification of proteins by scavenging carbonyl intermediates of carbohydrate and lipid degradation. J Biol Chem 2002;277:3397–403. [PubMed: 11729198]
32. Onorato JM, Jenkins AJ, Thorpe SR, Baynes JW. Pyridoxamine, an inhibitor of advanced glycation reactions, also inhibits advanced lipoxidation reactions. Mechanism of action of pyridoxamine. J Biol Chem 2000;275:21177–84. [PubMed: 10801874]
33. Amarnath V, Amarnath K, Matherson T, Davies SS, Roberts LJ. A Simplified Synthesis of Diastereomers of Levuglandin E2. Synthetic Communications 2005;35:397–408.
34. Chandra A, Srivastava SK. A synthesis of 4-hydroxy-2-trans-nonenal and 4-(3H) 4-hydroxy-2-trans-nonenal. Lipids 1997;32:779–82. [PubMed: 9252968]
35. Reany O, Gunnlaugsson T, Parker D. J Chem Soc Perkin Trans 2000;2:1819–1831.
36. Wu Y, Ahlberg P. On the formation of isoproplidenepyridoxines. Acta Chem Scand 1989;43:1009–1011. [PubMed: 2488260]
37. Yang D, Shih Y, Liu H. Chemical synthesis of stereospecifically labeled pyridoxamine 5'-phosphate. J Org Chem 1991;56:2940–2946.
38. Kalnitsky G, Hummel JP, Dierks C. Some factors which affect the enzymatic digestion of ribonucleic acid. J Biol Chem 1959;234:1512–6. [PubMed: 13654407]
39. Williams, CH, Jr. Chemistry and Biochemistry of Flavoenzymes. Muller, F., editor. CRC Press; Boca Raton, FL: 1992. p. 121-211.
40. Longmire AW, Swift LL, Roberts LJ 2nd, Awad JA, Burk RF, Morrow JD. Effect of oxygen tension on the generation of F2-isoprostanes and malondialdehyde in peroxidizing rat liver microsomes. Biochem Pharmacol 1994;47:1173–7. [PubMed: 8161346]
41. Metz TO, Alderson NL, Chachich ME, Thorpe SR, Baynes JW. Pyridoxamine traps intermediates in lipid peroxidation reactions in vivo: evidence on the role of lipids in chemical modification of protein and development of diabetic complications. J Biol Chem 2003;278:42012–9. [PubMed: 12923193]
42. Boutaud O, Aronoff DM, Richardson JH, Marnett LJ, Oates JA. Determinants of the cellular specificity of acetaminophen as an inhibitor of prostaglandin H(2) synthases. Proc Natl Acad Sci U S A 2002;99:7130–5. [PubMed: 12011469]
43. Lagarde M, Bryon PA, Guichardant M, Dechavanne M. A simple and efficient method for platelet isolation from their plasma. Thrombosis Research 1980;17:581–588. [PubMed: 7368178]
44. Bernoud-Hubac N, Davies SS, Boutaud O, Montine TJ, Roberts LJ 2nd. Formation of highly reactive gamma-ketoaldehydes (neuroketals) as products of the neuroprostane pathway. J Biol Chem 2001;276:30964–70. [PubMed: 11413140]

45. Crouch SP, Kozlowski R, Slater KJ, Fletcher J. The use of ATP bioluminescence as a measure of cell proliferation and cytotoxicity. J Immunol Methods 1993;160:81–8. [PubMed: 7680699]
46. Sayre LM, Arora PK, Iyer RS, Salomon RG. Pyrrole formation from 4-hydroxynonenal and primary amines. Chem Res Toxicol 1993;6:19–22. [PubMed: 8448343]
47. Stitt A, Gardiner TA, Alderson NL, Canning P, Frizzell N, Duffy N, Boyle C, Januszewski AS, Chachich M, Baynes JW, Thorpe SR, Anderson NL. The AGE inhibitor pyridoxamine inhibits development of retinopathy in experimental diabetes. Diabetes 2002;51:2826–32. [PubMed: 12196477]
48. Alderson NL, Chachich ME, Youssef NN, Beattie RJ, Nachtigal M, Thorpe SR, Baynes JW. The AGE inhibitor pyridoxamine inhibits lipemia and development of renal and vascular disease in Zucker obese rats. Kidney Int 2003;63:2123–33. [PubMed: 12753299]
49. Voziyan PA, Khalifah RG, Thibaudeau C, Yildiz A, Jacob J, Serianni AS, Hudson BG. Modification of proteins In vitro by physiological levels of glucose: Pyridoxamine inhibits conversion of amadori intermediate to advanced glycation end-products through binding of redox metal ions. J Biol Chem 2003;278:46616–46624. [PubMed: 12975371]
50. Price DL, Rhett PM, Thorpe SR, Baynes JW. Chelating activity of advanced glycation end-product inhibitors. J Biol Chem 2001;276:48967–72. [PubMed: 11677237]
51. Boutaud O, Brame CJ, Chaurand P, Li J, Rowlinson SW, Crews BC, Ji C, Marnett LJ, Caprioli RM, Roberts LJ 2nd, Oates JA. Characterization of the lysyl adducts of prostaglandin H-synthases that are derived from oxygenation of arachidonic acid. Biochemistry 2001;40:6948–55. [PubMed: 11389610]
52. Fuson KS, Mark RJ, Panetta JA, May PC. Characterization of LY231617 protection against hydrogen peroxide toxicity. J Neurochem 1999;72:1154–60. [PubMed: 10037488]
53. Sametz W, Hummer K, Butter M, Wintersteiger R, Juan H. Formation of 8-iso-PGF(2alpha) and thromboxane A(2) by stimulation with several activators of phospholipase A(2) in the isolated human umbilical vein. Br J Pharmacol 2000;131:145–51. [PubMed: 10960081]
54. Mark RJ, Fuson KS, May PC. Characterization of 8-epiprostaglandin F2alpha as a marker of amyloid beta-peptide-induced oxidative damage. J Neurochem 1999;72:1146–53. [PubMed: 10037487]
55. Hart CM, Karman RJ, Blackburn TL, Gupta MP, Garcia JG, Mohler ER 3rd. Role of 8-epi PGF2alpha, 8-isoprostane, in H2O2-induced derangements of pulmonary artery endothelial cell barrier function. Prostaglandins Leukot Essent Fatty Acids 1998;58:9–16. [PubMed: 9482161]
56. Salahudeen A, Badr K, Morrow J, Roberts J 2nd. Hydrogen peroxide induces 21-aminosteroid-inhibitable F2-isoprostane production and cytolysis in renal tubular epithelial cells. J Am Soc Nephrol 1995;6:1300–3. [PubMed: 8589301]
57. Ruef J, Moser M, Kubler W, Bode C. Induction of endothelin-1 expression by oxidative stress in vascular smooth muscle cells. Cardiovasc Pathol 2001;10:311–5. [PubMed: 11755377]
58. Yang CF, Shen HM, Ong CN. Protective effect of ebselen against hydrogen peroxide-induced cytotoxicity and DNA damage in HepG2 cells. Biochem Pharmacol 1999;57:273–9. [PubMed: 9890554]
59. Bai J, Rodriguez AM, Melendez JA, Cederbaum AI. Overexpression of catalase in cytosolic or mitochondrial compartment protects HepG2 cells against oxidative injury. J Biol Chem 1999;274:26217–24. [PubMed: 10473575]
60. Lennon SV, Martin SJ, Cotter TG. Dose-dependent induction of apoptosis in human tumour cell lines by widely diverging stimuli. Cell Prolif 1991;24:203–14. [PubMed: 2009322]
61. Hampton MB, Orrenius S. Dual regulation of caspase activity by hydrogen peroxide: implications for apoptosis. FEBS Lett 1997;414:552–6. [PubMed: 9323034]
62. Akao M, O'Rourke B, Teshima Y, Seharaseyon J, Marban E. Mechanistically distinct steps in the mitochondrial death pathway triggered by oxidative stress in cardiac myocytes. Circ Res 2003;92:186–94. [PubMed: 12574146]
63. Takeyama N, Miki S, Hirakawa A, Tanaka T. Role of the mitochondrial permeability transition and cytochrome C release in hydrogen peroxide-induced apoptosis. Exp Cell Res 2002;274:16–24. [PubMed: 11855853]

64. Long X, Goldenthal MJ, Wu GM, Marin-Garcia J. Mitochondrial Ca2+ flux and respiratory enzyme activity decline are early events in cardiomyocyte response to H2O2. J Mol Cell Cardiol 2004;37:63–70. [PubMed: 15242736]

Abbreviations Used

γKA
γ-ketoaldehydes

PM
pyridoxamine

SA
Salicylamine

PPM
5'-O-pentylpyridoxamine

IsoK
isoketal

HNE
4-hydroxynonenal

[^{3}H]-MeIsoK
methyl-[12-^{3}H]-15-E_2-isoketal

OVA
chicken egg ovalbumin

PBS
phosphate buffered saline

LC/MS/MS
HPLC coupled to tandem mass spectrometry

F_2-IsoP
F_2-isoprostanes

PGE_2
prostaglandin E_2

CID
collision-induced disassociation

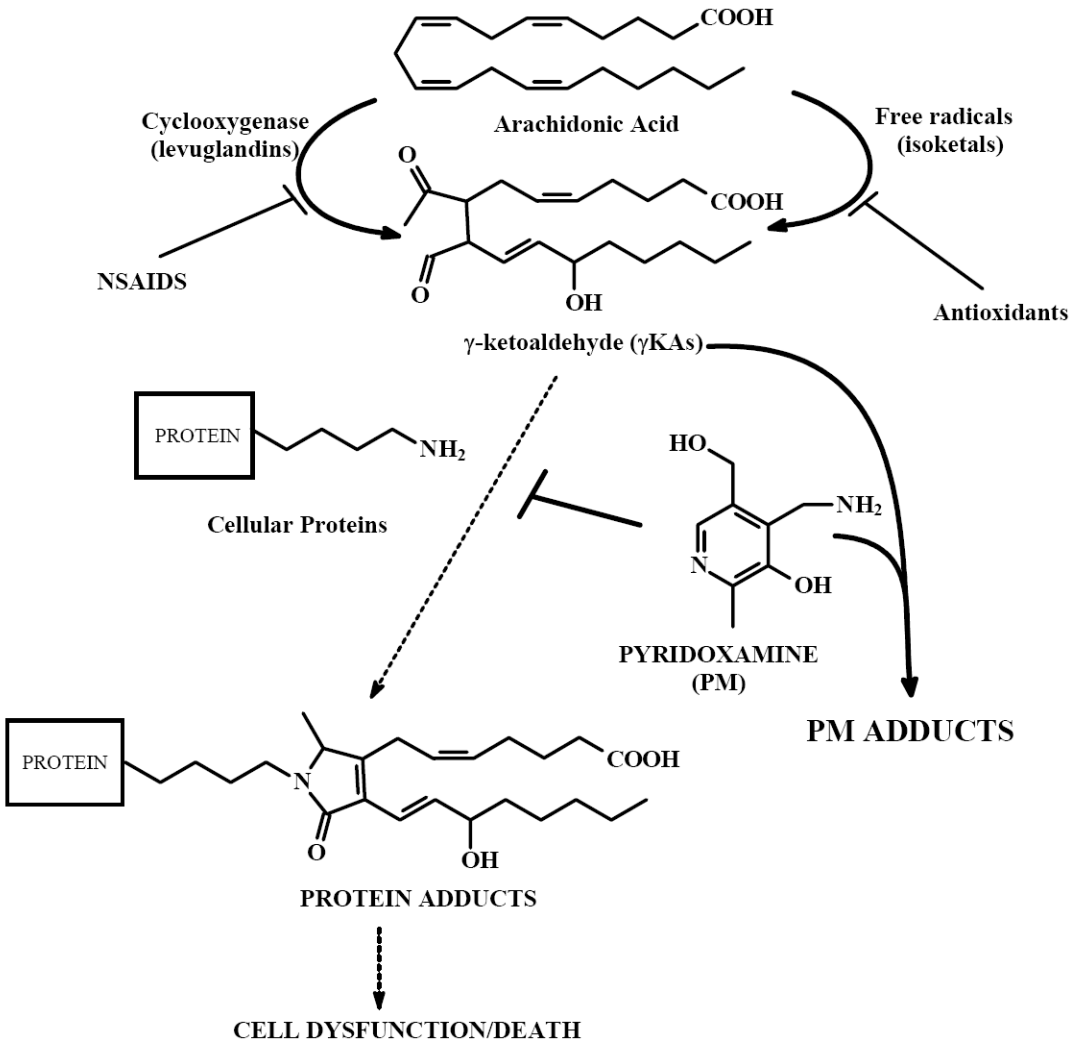

Figure 1.

Schematic of scavenging of γ-ketoaldehyde by pyridoxamine. Highly reactive γ-ketoaldehydes can be formed by two pathways during disease processes. Cyclooxygenases convert arachidonic acid to prostaglandin H_2, which rearranges non-enzymatically to form levuglandins E_2 and D_2, or is transformed enzymatically to form prostaglandins and thromboxane. Free radical mediated oxidation of arachidonic acid forms PGH_2 isomers, which similarly rearrange to form the isoketals, a series of 64 regio- and stereo-isomers of the levuglandins, as well as isoprostanes. Once formed, these γ-ketoaldehydes rapidly adduct to proteins, potentially altering their structure and function and leading to cell death. By rapidly reacting with these γ-ketoaldehyde to form stable adducts, pyridoxamine prevents the formation of protein adducts.

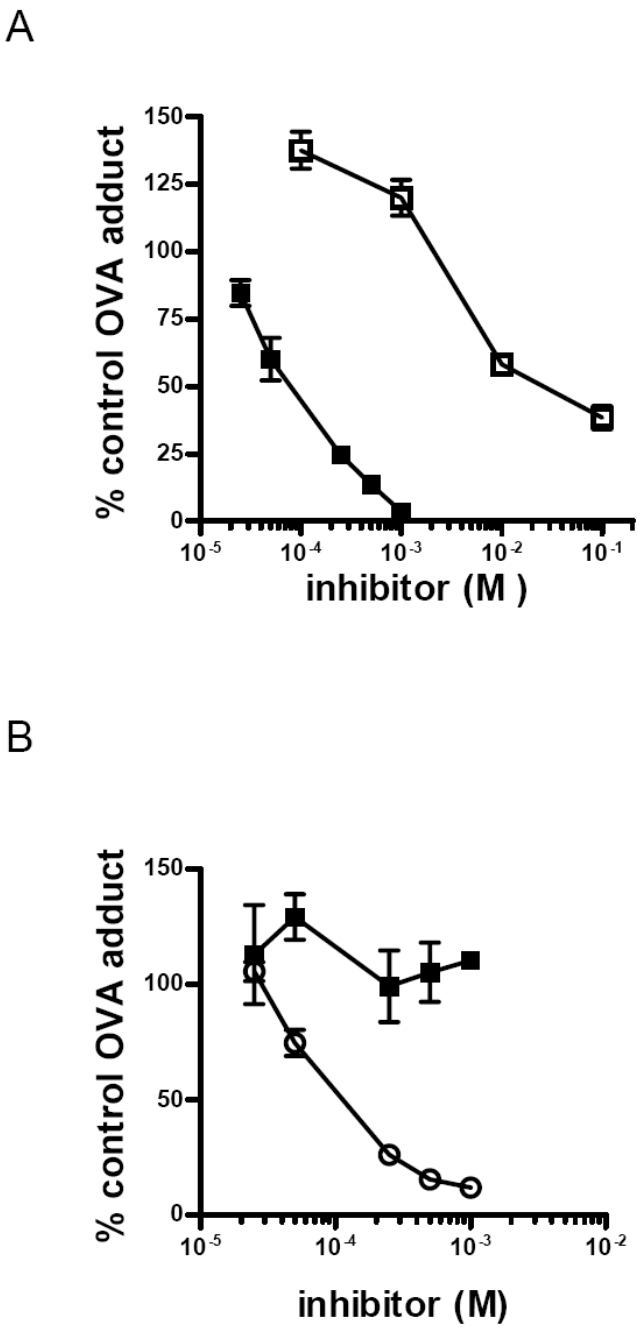

Figure 2.

Pyridoxamine protects proteins from adduction by γKA, but not HNE. OVA (10 μM) was incubated with 50 μM of either [^{3}H]-MeIsoK for 2 h or [^{3}H]-HNE for 24 h in the presence of various inhibitors. OVA was precipitated, washed, and the radioactivity counted. *A.* Percent of radioactivity precipitated with OVA incubated with [^{3}H]-MeIsoK in the presence of various concentrations of either pyridoxamine (-■-) or N^{α}-acetyllysine (-□-). (Mean±SEM, n = 3). *B.* Percent of radioactivity precipitated with OVA incubated with [^{3}H]-HNE in the presence of various concentrations of either pyridoxamine (-■-) or N^{α}-acetylcysteine (-○-). (Mean±SEM, n = 3).

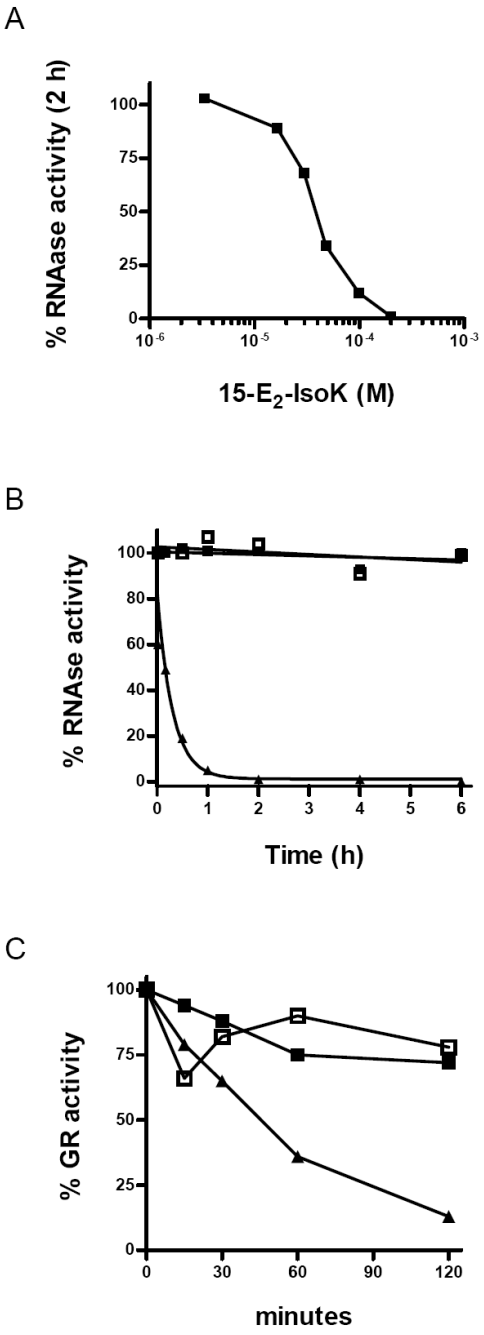

Figure 3.

PM protects enzymes from inhibition by γKA. *A.* The synthetic γKA, 15-E_2-IsoK inhibits activity of RNase A in a dose-dependent manner. RNase A (41 μg/ml) was incubated with 0-200 μM IsoK for 2 h and RNase A activity measured. *B.* PM protects RNase A from inhibition by IsoK. RNase A (41 μg/ml) and IsoK (200 μM) were incubated either in the absence (- ▲-) or presence (-■-) of 500 μM pyridoxamine. RNase A was also incubated with corresponding amount of vehicle (DMSO) (- □-). C. PM prevents inhibition of glutathione reductase by IsoK. Glutathione reductase (4.5 μg/ml) was incubated with vehicle (- □-) or IsoK (50 μM) either in the absence (- ▲-) or presence (-■-) of 200 μM PM.

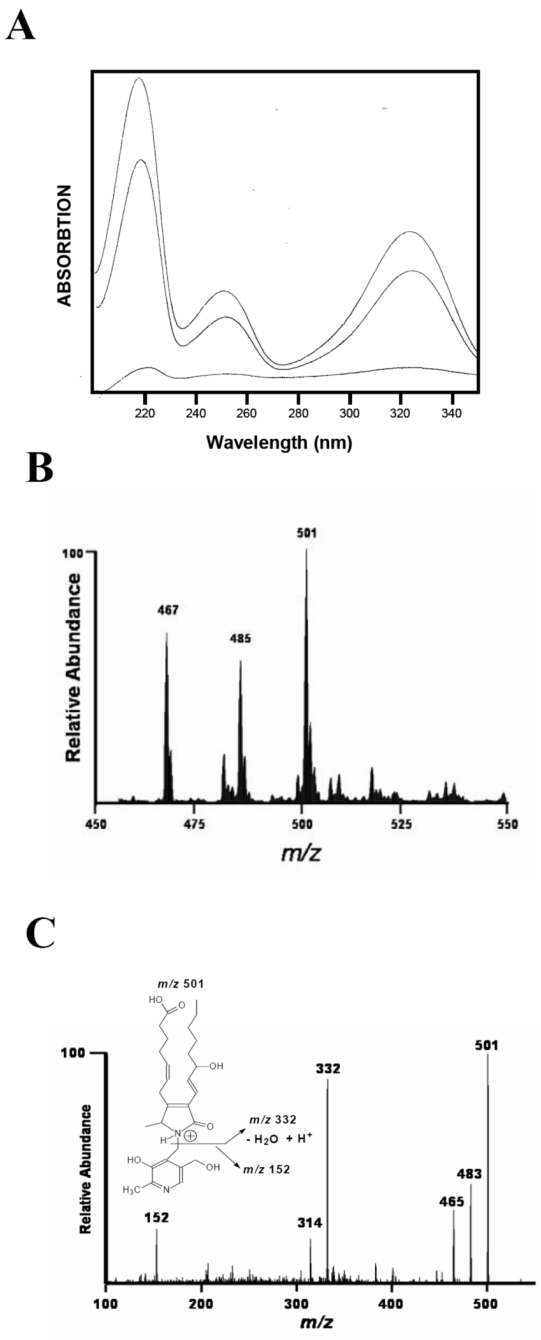

Figure 4.

PM reacts with IsoK to form a lactam adduct, as well as other products. 15-E_2-IsoK (250 μM) was reacted with PM (1mM) overnight. *A.* UV spectrometric scans of reaction solutions containing either IsoK (lower curve), PM (upper curve), or IsoK with PM (middle curve) reveals no shift in absorption maxima for PM after reaction with IsoK. *B.* ESI positive ion mass spectrometry mass scanning from *m/z 450* to *550* of the reaction products of IsoK with PM identify three major products peaks including *m/z 501*, the putative lactam product. Scans for solution with IsoK alone and with PM alone were subtracted to identify novel peaks present only in the reaction with IsoK and PM. *C.* Collision induced disassociation for *m/z 501* gives

signature product ion (*m/z 332*) for lactam adduct and PM (*m/z 152*), as well as peaks consistent with the loss of water molecules from the parent and product ions.

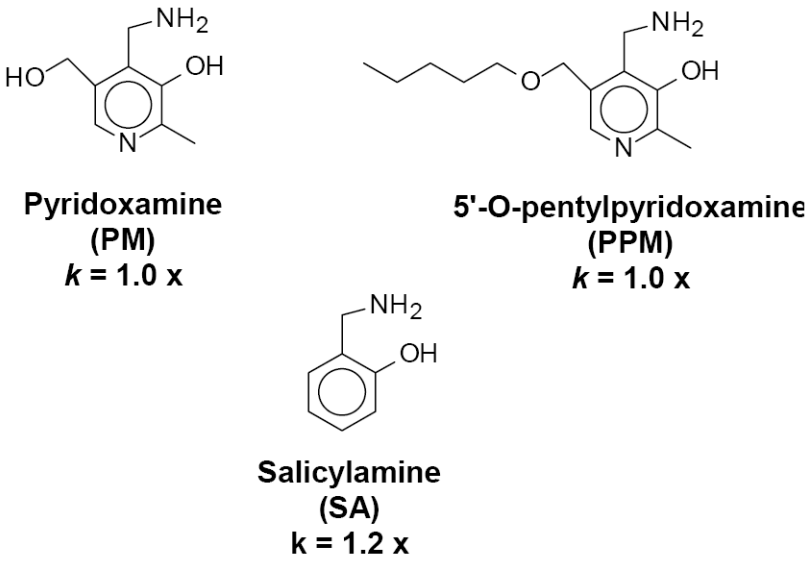

Figure 5.

PM and its lipophilic analogs. Pyridoxamine, Salicylamine, and 5'-O-pentylpyridoxamine all share a methylamine substituent adjacent to the phenolic group of the aromatic ring. The second order reaction rate (*k*) with the model γKA, 4-oxo-pentanal, are shown relative to PM.

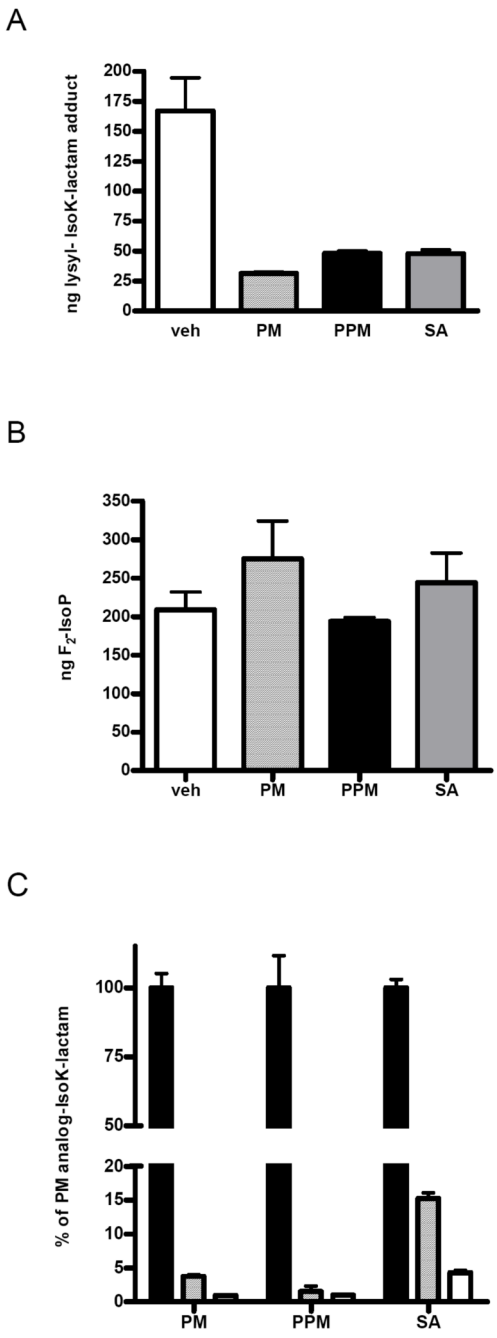

Figure 6.

PM analogs preferentially intercept γKA formed during oxidation of arachidonic acid to prevent lysyl adduct formation. Arachidonic acid was oxidized for two hours, then 1 mM lysine and either vehicle or 100 μM PM analog added. Twenty-two hours after the addition of the amines, the reaction products were analyzed by LC/MS/MS. *A.* Levels of lysyl-IsoK-lactam adduct formed (Mean±SEM, n = 3). Inclusion of 100 μM PM, PPM, or SA all significantly reduced the amount of adduct compared to the vehicle control ($p<0.01$, t test). *B.* Levels of F_2-isoprostanes, non-reactive products of the same lipid peroxidation pathway that form IsoKs, generated during arachidonic acid oxidation (Mean±SEM, n = 3). Inclusion of 100 μM PM, PPM, or SA did not significantly alter the amount of F_2-isoprostanes compared to the vehicle

control ($p>0.05$, t test). *C.* Amount of two putative α-ketoaldehyde adducts, *N*-pentanedioyl (dashed bars) and *N*-hexanoyl (open bars), formed relative to IsoK-lactam adduct (solid bars) formed in presence of individual PM analogs (Mean±SEM, n = 3).

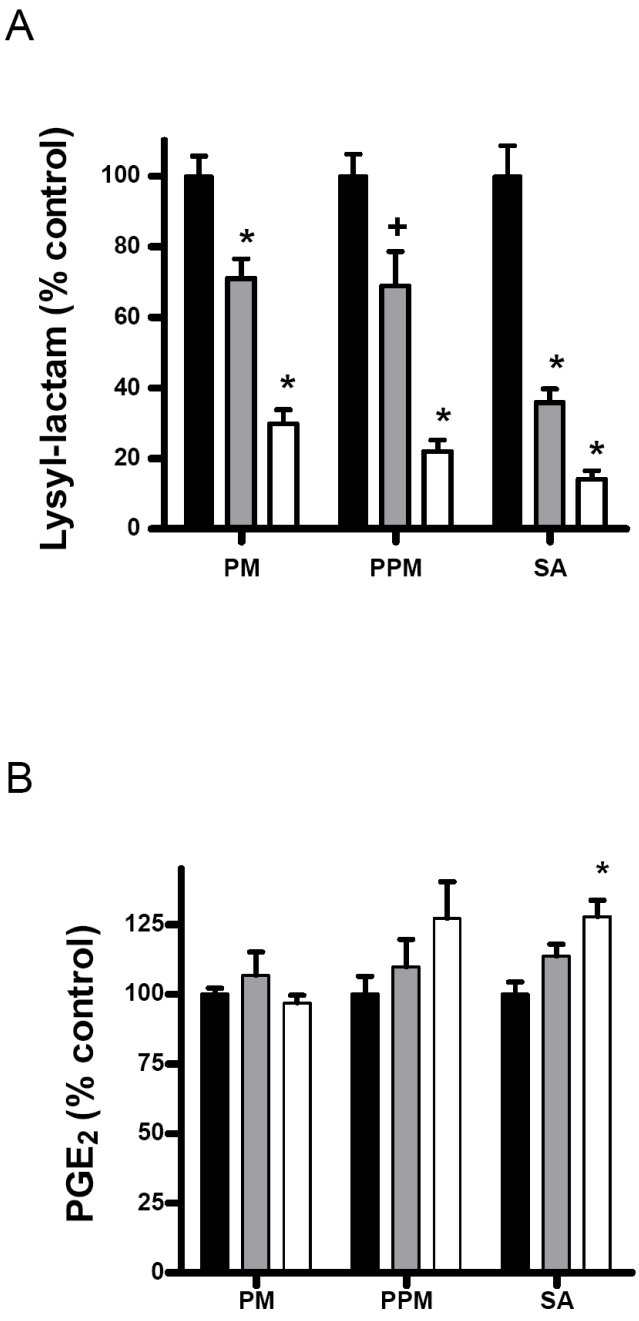

Figure 7.

PM analogs dose-dependently inhibit γKA adduct formation in platelets without inhibiting cyclooxygenase activity. Washed human platelets were preincubated with 10 μM dazoxiben and 0 μM (solid bars), 0.1 mM (shaded bars) or 1 mM (open bars) PM analog for 30 minutes. Arachidonic acid was then added to a final concentration of 20 μM. After 2 h the cells were pelleted, and lysyl-levuglandin- lactam protein adducts in the cell pellet were measured by LC/MS/MS after complete proteolytic digestion and the levels of PGE_2 in the supernatant were measured by GC/MS. *A.* Levels of lysyl-levuglandin- lactam adduct present in platelet pellet (Mean ±SEM; PM, n = 10 ; PPM, n = 4; SA, n = 8; $^{+}$ $p < 0.05$; * $p < 0.001$ Dunnet's post-test

after one-way ANOVA for individual PM analog) *B.* Levels of PGE_2 in the platelet supernatant (Mean ± SEM; * $p < 0.01$).

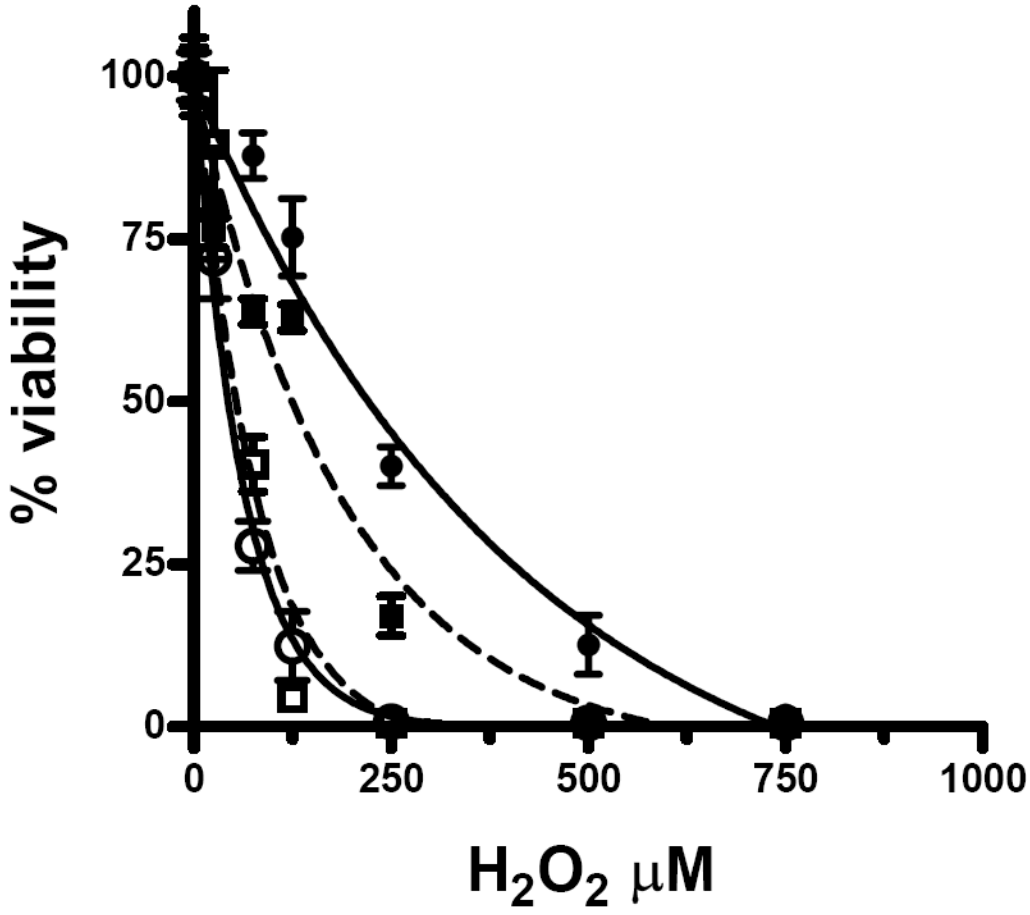

Figure 8.

Lipophilic PM analogs protect against H_2O_2-mediated cytotoxicity in HepG2 cells. HepG2 were plated in multiple 96-well plates at 2×10^4 cells per well and pretreated with vehicle only (- -□- -), 2 mM PM (—○—), 0.5 mM PPM (- -■- -), or 0.5 mM SA (—●—) for 45 minutes. Replicate wells were treated with 0, 25, 75, 125, 250, 500, or 750 μ^M H_2O_2 and cell viability after 24 hours determined by measuring ATP levels (Mean ± SEM, n = 8). Two-way ANOVA of vehicle treated cells vs each of the individual PM analogs showed a significant effect of pretreatment with SA ($p < 0.0001$) and PPM ($p < 0.0015$), but not with PM ($p = 0.333$).

TABLE 1

Amine	IsoK-lactam	N-pentandioyl	N-Hexanoyl
PM	m/z 501 → 152 (3.5 min)	m/z 283 → 152 (0.7 min)	m/z 267 → 152 (3.0 min)
SA	m/z 456 → 107 (3.6 min)	m/z 238 → 107 (2.2 min)	m/z 222 → 107 (3.3 min)
PPM	m/z 571 → 222 (4.1 min)	m/z 353 → 222 (3.1 min)	m/z 337 → 222 (3.9 min)

Precursor and product ions used for selective reaction monitoring of IsoK-lactam, *N*-pentanedioyl, and *N*-hexanoyl adducts of PM analogs. Retention times of peak integrated for each product are in parenthesis. The C18 Magic Bullet column volume = 25 μl (0.13 min).